Journal of Water Process Engineering 23 (2018) 265–276

Contents lists available at ScienceDirect

Journal of Water Process Engineering

journal homepage: www.elsevier.com/locate/jwpe

Improved barium removal and supersaturation depletion in wastewater by precipitation with excess sulfate

Flávia M. Ronquim[a,*], Marycel E.B. Cotrim[b], Sabine N. Guilhen[b], André Bernardo[c], Marcelo M. Seckler[a]

[a] Department of Chemical Engineering, Polytechnic School, University of São Paulo, Av. Prof. Luciano Gualberto, n. 380, trav. 3, 05508-900, São Paulo, SP, Brazil
[b] Institute of Energy and Nuclear Research, Av. Lineu Prestes 2242, São Paulo, SP, Brazil
[c] Department of Chemical Engineering, Federal University of São Carlos, Rod. Washington Luiz, km 235 – SP 310, 13565-905, São Carlos, SP, Brazil

ARTICLE INFO

Keywords:
Barium sulfate precipitation
Residual supersaturation
Excess sulfate addition
Calcium foreign ion
Heterogeneous seeding

ABSTRACT

Barium ions found in wastewaters cause incrustation on membrane separation equipment used in desalination systems. In this study barium removal by precipitation is addressed, considering excess sulfate addition as a means of reducing barium concentration in solution and depleting $BaSO_4$ supersaturation. Precipitation is conducted with synthetic wastewater in semicontinuous mode. For low excess sulfate, an induction time of a few hours is observed. As the excess sulfate is increased and/or as barium sulfate seeds are added, precipitation proceeds within a few minutes. Besides, the excess sulfate improves barium ion removal due to the common-ion effect. Residual supersaturation ratios were found to lie within the range of 1.1–3. These values were associated with a fourth order dependency of the molecular growth rate with the supersaturation ratio. Calcium carbonate and calcium sulfate dihydrate were found to be ineffective heterogeneous seeds to barium sulfate precipitation. Calcium ions were found to inhibit $BaSO_4$ precipitation, blocking the process at a high residual supersaturation ratio of 4–5. For a sufficiently large initial supersaturation, the solution approaches equilibrium after 180 min.

1. Introduction

Barium sulfate ($BaSO_4$) is found in rock formations and hence in surface, groundwater and in many industrial aqueous effluents. When such an effluent solution is treated aiming at water reuse, barium may precipitate causing scaling. Most often scaling occurs in the desalination step in a membrane separation system, such as reverse osmosis or reversal electrodialysis. $BaSO_4$ scaling jeopardizes pumps, damages membranes and clogs pipelines, often causing irreversible damage. Scaling takes place because the solution fed to membrane operations is usually supersaturated. Besides, the supersaturation further increases within the brine compartment of the membranes, because of the concomitant removal of pure water from the solution. In order to minimize scaling, feed solutions to membrane operations should display low barium concentration. Recommended feed concentration of barium for a membrane separation system may be as low as 15 μg/L in seawaters, 5 μg/L in brackish waters or even 2 μg/L if sulfuric acid is dosed to brackish waters [1]. However, barium concentrations found in superficial waters or wastewaters are in the order of hundreds of micrograms per liter [2–4], emphasizing the need to remove barium prior to membrane treatment. It is also desirable that the feed solution supersaturation be as low as possible, to reduce its scaling tendency. Therefore, any barium removal treatment should aim at depletion of both barium concentration and supersaturation.

In order to remove barium ions from solution, chemical softening may be applied upstream the membrane operation [2,5,6,3,7]. In this process, the pH is increased by base addition, thereby decreasing the solubility of $CaCO_3$ and inducing its precipitation. Barium is removed from the bulk solution together with $CaCO_3$ by a sorption process, such as isomorphic substitution within the $CaCO_3$ crystal lattice or by adsorption [8–10]. After solids separation, the solution is acidified to prevent $CaCO_3$ scaling. This process, however, may be quite expensive due to alkaline and acid reactants addition and may be inefficient for feed streams with low calcium and carbonate concentrations. To circumvent these problems, $BaSO_4$ precipitation may also be conducted without reactants and independently of the amount of calcium and carbonate in the feed solution, by seeding with barite crystals, as shown by Bremere et al. [11] and Bremere et al. [12] in a fixed bed reactor and by Kügler et al. [13] in a mixed vessel. However, the residual barium concentration after seeding may be still too high considering its potential to promote scaling in downstream membrane operations.

In order to circumvent the inconveniences of Ba^{2+} removal by

* Corresponding author.
E-mail address: flaviamr@usp.br (F.M. Ronquim).

https://doi.org/10.1016/j.jwpe.2018.04.007
Received 3 November 2017; Received in revised form 20 March 2018; Accepted 7 April 2018
Available online 24 April 2018

softening and by seeding, the addition of sulfate ions may be an attractive option. Due to the common ion effect, the final Ba^{2+} concentration may be reduced, in principle, to a very low value by appropriate choice of the sulfate-to-barium molar ratio. Besides, supersaturation depletion to near-equilibrium is feasible, as will be shown here. In order to develop such a process option for processing of wastewater, one has to understand the precipitation of $BaSO_4$ under highly non-stoichiometric conditions. In the literature, the sulfate-to-barium molar ratio is rarely higher than 10:1. Boerlage et al. are one of the few scholars who have analyzed the $BaSO_4$ precipitation for a sulfate-to-barium molar ratio of 1000:1, which corresponds to conditions found in surface waters and industrial effluents. They have investigated barium sulfate solubility [14], as well as nucleation and growth kinetics [15] in experiments with industrial and synthetic reverse osmosis concentrates. They have concluded that long induction times associated to scale formation in reverse osmosis are due to the low kinetics of $BaSO_4$ precipitation. They have also found that organic matter neither prolongs the induction time nor influences $BaSO_4$ solubility, but it does impair crystal growth rates. A high $BaSO_4$ non-stoichiometry has been found to lower the growth rate.

As calcium ions are always present in wastewaters, it is useful to consider its influence on $BaSO_4$ precipitation. In the absence of "organic additives", Ca^{2+} retards the precipitation of $BaSO_4$ [16]. According to Jones et al. [17], calcium concentrations up to 2.5×10^{-4} M delays barium sulfate formation by an ionic strength effect, which increases the $BaSO_4$ solubility and decreases its supersaturation. Above 1.25×10^{-3} M calcium (for Ba:SO_4 in stoichiometric ratio), crystallization is inhibited beyond the expected from the ionic strength effect alone. In this case, incorporation of calcium may occur in the crystalline structure of $BaSO_4$, causing an increase of the crystal internal energy (making it more soluble and unstable) and/or may occur on the $BaSO_4$ surface, poisoning the crystal growth [17]. Indeed, barium sulfate can support up to 6% calcium substitution for barium ions in its crystal lattice (Grahmann cited by Hennessy and Graham [18]. Kelland [19] has also found that calcium ions inhibit the precipitation of $BaSO_4$, while Redfern and Parker [20] have detected by atomistic simulations that $CaSO_4$ overgrowth upon $BaSO_4$ crystals is energetically unfavorable. They have noticed deformations caused by calcium on the crystalline structure of $BaSO_4$, with high effect on surface energy.

In general, literature for barium sulfate precipitation from non-stoichiometric solutions focuses on the particle size distribution, the mean particle size, the particle morphology [21–25], and on the precipitation kinetics [26–30]. Contributions dealing with barium sulfate for water treatment usually consider the percent barium removal and the barium concentration of the treated water. However, little attention has so far been paid to the residual supersaturation after treatment. Bremere et al. [11] have determined the supersaturation depletion in seeded $BaSO_4$ precipitation, whereas Metzger and Kind [31] have calculated the supersaturation depletion from a computational fluid dynamics approach for $BaSO_4$ precipitation in a confined impinging jet mixer.

To the authors' knowledge, no contribution has been found so far about $BaSO_4$ precipitation time for conditions of high sulfate-to-barium ratio and presence of calcium foreign ions or barium sulfate seeds. Therefore, these conditions, which are relevant for wastewater treatment, will be explored next. The sulfate-to-barium molar ratio will vary within the molar range of 1:500 to 1:46300, the calcium concentration will vary within the range of 1.75×10^{-3} to 5.37×10^{-3} M. $BaSO_4$ precipitation in the presence of barium sulfate seeds and of heterogeneous particles ($CaCO_3$ and $CaSO_4$) will be considered as well. The ionic strength will be within the range of 0.003–0.313 M to mimic conditions found in wastewaters. Barium sulfate precipitation will be analyzed in terms of equilibrium, mechanistic and kinetic considerations. Process performance in relation to the scaling potential of the treated water will be addressed in terms of the barium concentration and the residual supersaturation of the treated water.

2. Background

2.1. Thermodynamics of precipitation

The supersaturation ratio (S) represents the driving force for the precipitation process. In a solution containing $BaSO_4$, S may be calculated by Eq. (2), where the brackets indicate the ionic molar concentration, γ is the activity coefficient, K_{ps} represents the thermodynamic solubility product of barium sulfate, $K_{ps} = 1047 \times 10^{-10}$ M^2 (NIST 46.7 [32]); "*a*" is the activity and, finally, the subscripts "eq" refer to thermodynamic equilibrium (S = 1).

$$S = \sqrt{\frac{\gamma + [Ba^{2+}]\gamma - [SO_4^{2-}]}{K_{ps}}} = \sqrt{\frac{{}^{a}Ba^{2+\,a}\ SO_4^{2-}}{{}^{a}Ba^{2+},\ eq^{\,a}\ SO_4^{2-},\ eq}} \tag{2}$$

Although the activity coefficient γ_i refers to an ionic species i, in this case, $\gamma_{\pm} = (\gamma_+\gamma_-)^{1/2}$ is the mean ionic activity coefficient, which is calculated using the Davies equation (Eq. (3)). The first term of the equation represents the long-range ionic interaction following Coulomb's force between oppositely charged ions, where A is the Debye-Hückel constant ($A = -0$, 5079 to 25 °C), $z_{\pm,i}$ is the ionic charge for species *i* in solution and *I* is the ionic strength. The second term (linear in relation to the ionic strength) improves the empirical fit for high ionic strength, but has no theoretical justification.

$$\log \gamma_{\pm} = Az_{\pm}^{2}\left[\left(\frac{\sqrt{I}}{1+\sqrt{I}}\right) - 0{,}3I\right] \tag{3}$$

The ionic strength *I* is defined by Eq. (4), where $[_i]$ is the concentration of each species *i* in solution [mol L^{-1}].

$$I = \frac{1}{2}\sum_{n}^{i=1} [_i]z_i^{\,2} \tag{4}$$

According to Oncul et al. [33], Eq. (3) may be applied to I values as high as 0.6.

The activities of the free ions Ba^{2+} and SO_4^{2-} in solution required in Eq. (2) depend on the concentrations of other species in solution, such as ions and complexes. In $BaSO_4$ precipitation carried out by mixing aqueous solutions of Na_2SO_4 and $BaCl_2$ the complexes $BaSO_{4(aq)}$, $BaCl^+$, $NaSO_4^-$ e $NaCl_{(aq)}$ are formed. Their concentration increase in the presence of other electrolytes such as NaCl. Vicum et al. [34] identified an increase of the complex $BaSO_{4(aq)}$ formation for non-stoichiometric sulfate-to-barium ratio and for close-to-stoichiometry conditions with high levels of supersaturation. The $BaSO_{4(aq)}$ complex derives from the chemical reaction:

$$Ba^{2+}{}_{(aq)} + SO_4^{2+}{}_{(aq)} \leftrightarrow BaSo_{4(aq)}$$

The formation constant for this reaction $K_{BaSO4(aq)}$ is given by:

$$K_{BaSO_{4(aq)}} = \frac{\gamma_{BaSO_4(aq)}[BaSO_{4(aq)}]}{\gamma_+[Ba^{2+}]\gamma_-[SO_4{}^{2-}]} \tag{5}$$

With $K_{BaSO_{4(aq)}} = 134.89$. For other complexes analogously defined formation constants are $K_{BaCl^+} = 0.933$, $K_{NaSO_4^-} = 5.495$ and $K_{NaCl_{(aq)}} = 0.501$ (NIST 46.7 [32]) at 25 °C. For barium sulfate precipitation in the presence of other components such as calcium and carbonate, additional species and ion pairs are formed. In such cases, the speciation model in MINTEQ 3.1® software may be conveniently applied for determination of the supersaturation ratio S.

2.2. Barium sulfate nucleation

The primary nucleation rate, B, in $\#s^{-1}\,m^{-3}$, represents the number of nuclei generated in a unit time interval per unit solvent volume:

$$B = K'exp\left(\frac{-\Delta G}{kT}\right) \tag{7}$$

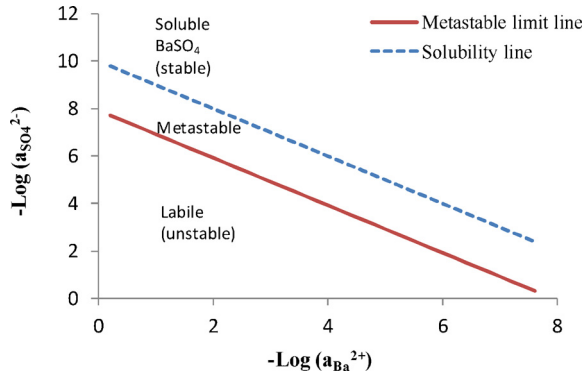

Fig. 1. Solubility and metastable zone limit for $BaSO_4$. The metastable limit line was drawn considering $(a_{Ba^{2+}})(a_{SO_4^{2-}}) = 115.2K_{ps}$. This equation comes from the one proposed by Cobbett and French [36]: $[SO_4^{2-}][Ba^{2+}] = 160\,K_{ps,}$ where the concentration was converted to activity using the MINTEQ software. With Kps = $1.047 \times 10^{-10}\,M^2$.

where K' is the nucleation rate constant and k is the Boltzmann constant. ΔG is the Gibbs free energy change to form a nucleus [35], given by:

$$\Delta G = \frac{-16\pi\gamma^3 V_m^2}{3k^2T^2(lnS)^2} \tag{8}$$

where γ represents the interfacial free energy of formation of the cluster, V_m is the molecular volume and T is the temperature. The primary nucleation rate, B, is critically dependent on the supersaturation, as Eqs. (7) and (8) show. It is a random unpredictable phenomenon with low probability at low supersaturation. Therefore, although primary nucleation is thermodynamically feasible at any supersaturation, a critical level of supersaturation is required for crystallization to occur spontaneously within a specified timescale. For barium and sulfate in stoichiometric proportions in water, an S of 10.2 is estimated from literature data [36]. Such critical level may be represented by the so-called metastable limit line in the phase diagram, as shown in Fig. 1. The region of the phase diagram located between this line and the solubility line is known as the metastable zone. In this region, primary nucleation is unlikely; only crystal growth and sometimes secondary nucleation takes place [35]. In the region above the metastable zone limit, called the labile zone, spontaneous primary nucleation occurs.

The induction time is defined as the time elapsed between the creation of supersaturation and the appearance of the new solid phase of a detectable macroscopic volume.

2.3. Barium sulfate crystal growth rate

Slightly soluble electrolytes such $BaSO_4$ at low supersaturation grow primarily by a spiral growth mechanism. As supersaturation increases, 2D nucleation-mediated growth becomes dominant. For even higher values of supersaturation, diffusion becomes the controlling mechanism for crystal growth [37]. The relationships between the rate of linear growth G_{lin} and the supersaturation ratio S for these mechanisms are given by Eqs. (9) and (10), where L is the crystal size, k_g is the growth rate constant, which is independent of S and directly related to the solubility, g is growth order and B_{2D} is the surface nucleation rate.

$$G_{lin} = \frac{dL}{dt} = k_g(S-1)^g \tag{9}$$

$$G_{lin} = k_g(S-1)^{\frac{2}{3}}S^{\frac{1}{3}}exp\frac{-B_{2D}}{lnS} \tag{10}$$

Eq. (9) with $g = 2$ represents spiral growth, whereas $g = 1$ is applicable to diffusion controlled growth. Eq. (10) is applied to 2D nucleation-mediated growth. For simplicity, the 2D nucleation mediated growth rate may be represented by Eq. (9) considering g an "effective order" of the growth process, usually $g > 2$, so all growth mechanisms may be expressed by Eq. (9). Table 1 shows the crystal growth mechanisms for the $BaSO_4$-H_2O system, which prevail for the given ranges of S and of the surface area of seeds, A_{seed} (m^2/L) or seeds concentration C_{seed} (mg/L).

Table 1
Crystal growth mechanisms for the $BaSO_4$-H_2O system.

Growth mechanisms	Barium Sulfate		
	S	g	Reference
Spiral growth	S = 1.86 for C_{seed} > 285 mg/L[a]	2	[27]
	3.11 ≤ S ≤ 4.94	2	[15]
	S < 6	2	[38]
	S < 6.18 for A_{seed} > 0.430 m^2/L[b]	2	[39]
2D nucleation-mediated growth	S = 1.86 for C_{seed} = 28 mg/L	20	[27]
	S = 3.74	3	[40]
	4.54 ≤ S ≤ 11.04	3–6	[41]
	S ≥ 6.18 for A_{seed} < 0.430 m^2/L[b]	3–4	[39]
	17.11 ≤ S ≤ 46.9[c]	3	[42]
	S < 32.5[d]	4	[43]
Diffusion controlled growth	S > 6	1	[38]
	S > 32.5[d]	1	[43]

For relatively low values of supersaturation ratio (usually S < 6) van Leeuwen [38] has grown $BaSO_4$ by spiral growth, yielding g = 2 and $k_g = 2.8 \times 10^{-10}$. Boerlage et al. [15], with non-stoichiometric concentrations (SO_4^{2-}/Ba^{2+} molar ratio of about 1000) has found g = 2 but a smaller growth constant of $k_g = 4.9 \times 10^{-14}$. As the supersaturation ratio increases (typically 4 < S < 32), 2D-nucleation-mediated growth mechanism with a variety of reaction growth orders (3 ≤ g ≤ 6) have been reported. For Nancollas and Purdie [27] and Liu et al. [39] however, besides the supersaturation, a low amount of added seeds (A_{seed} < 0.430 m^2/L) leads to a mechanism of surface nucleation. Liu et al. [39] have observed, for S > 6.18, an initial period of 5 min with fast crystal growth. During this period, the effective growth order g is between 3 and 4 as might be expected for a 2D-nucleation-mediated growth process. Thereafter, under low supersaturation, a spiral growth mechanism (g = 2) prevails. Nielsen [43] has reported a reaction order of g = 4 for S up to 32.5, whereas for S > 32.5 the controlling mechanism is volume diffusion. For supersaturation ratios up to a limit of S = 6 van Leeuwen [38] has considered spiral mechanism, but above this limit the mechanism changes straight to diffusion control with g = 1 and $k_g = 1.4 \times 10^{-9}$.

2.4. Crystal size and solubility

Molecules on the surface of a crystal do not have complete and homogeneously satisfied intermolecular interactions, so it can be said that they are in a state of tension. Considering the pressure in the crystal and in the liquid phase as p^c and p^f, respectively, when the crystal radius (r) decreases, p^c increases, also rising the crystal surface energy (σ_{sl}). Consequently, small crystals are more soluble than the large ones. This effect, which is significant for crystals in the submicron size range, is expressed by the Ostwald-Freundlich equation:

$$\frac{x_{eq}(r)}{x_{eq}(\infty)} = exp\frac{2\sigma_{sl}v_c}{rRT} \tag{11}$$

Where:

R = gas constant [kg m^2/(mol K s^2)]
T = absolute temperature [K]
$v_c = \rho_{BaSO_4}/M_{BaSO_4}$ = crystal molar volume [m^3/mol].
$x_{eq}(r)$ = solubility of an "r" radius particle [activity]
$x_{eq}(\infty)$ = equilibrium solubility [activity]

3. Mathematical model for $BaSO_4$ precipitation

A mathematical model has been developed to describe semi-continuous seeded $BaSO_4$ precipitation. Eq. (12) gives the population balance for crystals in the crystallizer, considering that the growth rate is independent of the crystal size and neglecting crystal agglomeration and breakage [44]. The crystallizer volume changes due to the sulfate reactant added in the beginning of the run.

$$\frac{\partial(nV)}{\partial t} + G\frac{(\partial nV)}{\partial L} = 0 \tag{12}$$

With the following initial and boundary conditions:
$n(L,0) = n_0(L)$
$n(0,t) = B/G$
In which:
$n(L,t)$ = number based population density [m^{-4}]
$n_0(L)$ = number based population density of seeds [m^{-4}]
V = suspension volume [m^3]
L = crystal size [m]
t = time [s]
G = linear growth rate [m/s]
B = nucleation rate [$\#/(m^3\ s^1)$]

The population balance Eq. (12) may be conveniently transformed into the following set of *j* ordinary differential equations in terms of the so-called moments of the particle size distribution $m_0 \ldots m_j$ [35]:

$$\frac{\partial(Vm_0)}{\partial t} = VB \tag{13}$$

$$\frac{\partial(Vmj)}{\partial t} = V\left(Gm_{j-1} + BL_N^j\right)\ \ (j = 1, 2, 3\ldots); \tag{14}$$

In which $m_j = \int_x^0 nL^j dL$ with units [m^{j-3}] is the j^{th} moment of the particle size distribution, L_N is the size of secondary nuclei. The initial conditions are given by the moments of the seeds size distribution:

$$m_0(t=0) = m_{0,seeds};\ m_1(t=0) = m_{1,seeds} \ldots\ m_j(t=0) = m_{j,seeds}.$$

The moments m_0 and m_1 represent, per unit of volume suspension, respectively the number of particles [$\#/m^3$] and the total length of the particles [m/m^3]; the quantity $k_a{\cdot}m_2$ gives the particles surface area [m^2/m^3] and the quantity $k_v{\cdot}m_3$ is the volume of particles [m^3/m^3]. Higher moments m_j, $j > 3$ do not have a straightforward physical meaning.

The presence of seeds and the slow sulfate solution feed rate are thought to prevent the solution from exceeding the metastable limit, so primary nucleation is neglected (B = 0). Secondary nucleation is also neglected as the solids content is low and the particles are small. The crystal growth rate is given by Eq. (9) with known kinetic parameters. The supersaturation ratio *S* is determined from mass balances as explained later. For the calculation of the moments m_0, m_1, m_2 e m_3, Eqs. (13) and (14) have been discretized, yielding Eqs. (15) below.

$$m_0(t) = m_0(t - \Delta t) + B.\ \Delta t \tag{15}$$

$$m_1(t) = m_1(t - \Delta t) + G.\ m_0(t).\ \Delta t \tag{16}$$

$$m_2(t) = m_2(t - \Delta t) + 2G.\ m_1.\ \Delta t \tag{17}$$

$$m_3(t) = m_3(t - \Delta t) + 3G.\ m_2.\ \Delta t \tag{18}$$

Considering a Na_2SO_4 feed stream and an initial solution of $BaCl_2$ and NaCl, mass balances for sodium, sulfate, barium and chloride in solution are given in Eqs. (19) through (22). In order to determine $C_{Ba}(t)$, $C_{SO4}(t)$, $C_{Na}(t)$ and $C_{Cl}(t)$, these equations have been discretized as before (not shown).

$$\frac{\partial(C_{Ba}V_{sol})}{\partial t} = -\rho_{BaSO4}.G.\ k_a.\ m_2.\ V.\ \frac{1}{MW_{BaSO4}} + C_{Ba,reag}.\ Q_{reag} \tag{19}$$

$$\frac{\partial(C_{SO4}V_{sol})}{\partial t} = -\rho_{BaSO4}.G.\ k_a.\ m_2.\ V.\ \frac{1}{MW_{BaSO4}} + C_{SO4,reag}.\ Q_{reag} \tag{20}$$

$$\frac{\partial(C_{Na}V_{sol})}{\partial t} = C_{Na,reag}.\ Q_{reag} \tag{21}$$

$$\frac{\partial(C_{Cl}V_{sol})}{\partial t} = C_{Cl,reag}.\ Q_{reag} \tag{22}$$

Where:

C_{Ba}, C_{SO4}, C_{Na} and C_{Cl} = component concentration in solution [mol/m^3]

$C_{Ba,reag}$, $C_{SO4,reag}$, $C_{Na,reag}$ and $C_{Cl,reag}$ = component concentration in reactant [mol/m^3].

ρ_{BaSO_4} = $BaSO_4$ seeds density [kg/m^3]
k_a = area shape factor of $BaSO_4$ seeds
MW_{BaSO4} = $BaSO_4$ molecular mass [kg/mol]
Q_{reag} = reactant flow rate [m^3/s]
V_{sol} = volume of solution in the crystallizer [m^3]

For this process, $V_{sol}(t)$ and $V(t)$ may be obtained by discretization of the following mass balances equations:

$$\frac{\partial(V_{sol})}{\partial t} = (\rho_{reag}/\rho_{sol})Q_{reag} \tag{23}$$

$$\frac{\partial(V)}{\partial t} = (\rho_{reag}/\rho_{susp})Q_{reag} \tag{24}$$

Barium and sulfate speciation in solution leads to the following additional mass balances (Eqs. (21) and (22)).

$$C_{Ba} = [Ba^{2+}] + [BaSO_{4(aq)}] + [BaCl^+] \tag{21}$$

$$C_{SO4} = [SO_4{}^{2-}] + [BaSO_{4(aq)}] + [NaSO_4{}^-] \tag{22}$$

An additional equation is needed to assure electroneutrality, i.e. the sum of positive and negative charges in solution should be zero (not shown). The distribution of barium and sulfate species obey the equilibrium relations given in Eq. (5) with activity coefficients determined with the Davies model (Eqs. (3) and (4)). The $BaSO_4$ supersaturation ratio (S) is calculated with Eq. (2), using the just determined free ions concentrations and activity coefficients.

4. Experimental

4.1. Precipitation equipment and procedure

Precipitation experiments were conducted in semi-continuous mode. Initially, the reactor was filled with 400 mL of a solution prepared with $BaCl_2{\cdot}2H_2O$, NaCl and, in some cases, $CaCl_2.2H_2O$. Seeds of $BaSO_4$, $CaCO_3$ or $CaSO_4{\cdot}2H_2O$ were allowed to equilibrate with the solution in the reactor during 20 min prior to reactant addition. The reaction was initiated by slowly pumping 100 mL of Na_2SO_4 aqueous solution through an inlet pipe at a flow rate of 0.83 mL/s. The final volume of solution was 500 mL. All reagents were analytical grade. The suspension was stirred at 300 r.p.m and the temperature was 25 °C.

The bench scale unit comprised a cylindrical rounded bottom jacketed glass reactor, with 1L volume and 10 cm diameter, a thermostatic bath (Quimis – Q214S) and an agitation system (IKA – RW20.N) with four 45° pitched blade impellers of 5 cm in diameter and positioned at 2 cm from the crystallizer bottom. A peristaltic pump (Provitec DM 5900 AX-D) fed the sulfate solution to the reactor through a pipe with 0.3 mm in internal diameter which ended at the same depth as the stirrer blades.

4.2. Sampling and analysis

In all experiments, samples of crystallization suspensions were collected with disposable syringes (10 mL). Several samples were withdrawn in each experiment, in order to follow the precipitation of $BaSO_4$

over the reaction time. The filled syringes were connected to disposable filters (GVS) of cellulose acetate with 25 mm in diameter and a pore size of 0.20 μm. In order to wash the filter, 2 mL of solution were filtered and discarded. Thereafter, 8 mL of solution were filtered and stored in falcon tubes (15 mL). Each falcon tube was then acidified with three or four droplets of concentrated nitric acid 65% P.A. and stored at 10 °C for chemical analysis. The acidification procedure was considered sufficient to keep the barium in solution since the presence of solids in the samples would heavily interfere with the reproducibility of ICP analysis or even prevent measurement by clogging of capillaries of the instrument, which has never been observed. Besides, in some situations the measurements matched the known initial concentrations, which would not happen in case of precipitation.

Precipitation of $BaSO_4$ was followed by determining the barium concentration in solution over time. Quantitative analysis was made by Inductively Coupled Plasma Spectrophotometry (Spectroflame). Chemical equilibria for determination of supersaturation ratios S and solution compositions were calculated with Visual MINTEQ 3.1® software.

4.3. Experimental conditions

Semi-continuous precipitation experiments were conducted with barium and sodium chloride concentrations similar to those commonly found in aqueous effluents of oil refineries. Sulfate concentrations intentionally exceeded commonly found values (here 110 mg/L is taken as a representative value) in order to promote Ba precipitation by the common ion effect. Tables 2 and 3 show the initial concentrations and the initial nominal concentrations of all ions, respectively. Both definitions are based on process conditions after reactant addition assuming no precipitation. However, initial values disregard contribution from seeds dissolution, whereas nominal values take seeds dissolution into account. Table 3 shows initial nominal ionic strength, sulfate-to-barium and calcium-to-barium molar ratios in solution and initial nominal supersaturation ratios S. For unseeded experiments, the initial and initial nominal S coincide, since there is no increase of the concentrations values by seeds dissolution. For seeded experiments, the initial nominal S is larger than the initial S due to seeds dissolution. However, the initial nominal S is equal to the actual initial S only when the induction time is longer than the time for reactants addition. Otherwise, the initial nominal S is higher the actual value.

4.4. Seeds characterization

In most batches, $BaSO_4$ seed crystals were aged in a solution containing $BaCl_2{\cdot}2H_2O$ and NaCl for 20 min prior to precipitation. $CaCO_3$ and $CaSO_4{\cdot}2H_2O$ seeds were added to 60 mL Milli-Q water without agitation for seven days prior to use. $BaSO_4$ seeds in the reactor were suspensions of 1 or 10 g/L. Calcite and Gypsum seeds were 0.3125 g/L $CaCO_3$ and 2.5810 g/L $CaSO_4{\cdot}2H_2O$ suspensions. These suspension densities yielded the same superficial area as 1 g/L of $BaSO_4$ after correction for the particles size and solubility.

Mean specific particle surfaces were estimated from images (Fig. 2) taken with a Field Emission Scanning Electron Microscope (JEOL, JSM-7401F). They were $8.33 \times 10^{-11}\ m^2$ for analytical grade $BaSO_4$, $1.42 \times 10^{-11}\ m^2$ for $CaCO_3$ and $4.13 \times 10^{-10}\ m^2$ for $CaSO_4.2H_2O$.

Table 2
Initial conditions of experiments. Solution concentrations disregard contribution from seeds dissolution.

Code	SO_4 (mg/L)	Ba (μg/L)	Ca (mg/L)	Added NaCl (mg/L)	$BaSO_4$ seed (g/L)	$CaCO_3$ seed (g/L)	$CaSO_4$ seed (g/L)
A, B	110.0	300	0	584	1	0	0
C	110.0	300	0	584	10	0	0
D	110.0	300	0	0	1	0	0
F	1070.6	300	0	584	1	0	0
I	9716.3	300	0	584	1	0	0
K	1070.6	330	0	584	0	0.3125	0
L	1070.6	362	0	584	0	0	2.5810
M	9716.3	300	0	584	0	0	0
N	9716.3	300	0	584	0	0	0
O	1070.6	400	0	584	0	0	0
P	1070.6	300	70	409	1	0	0
Q	1070.6	300	215	0	1	0	0
R	2372.7	300	70	584	1	0	0
S	9716.3	300	215	584	1	0	0

5. Experimental results

5.1. Excess sulfate

Semi-continuous barium sulfate precipitation by sulfate addition was studied. The initial barium concentration varied within the range of 300–400 μg/L and the background electrolyte sodium chloride concentration was 584 mg/L, while the sulfate concentration underwent a wide variation (Tables 2 and 3, experiments O, N and M). No seeds were present. Fig. 3a shows the soluble barium concentration during the precipitation reaction versus time. For an initial SO_4 concentration of 1070 mg/L, corresponding to a supersaturation ratio S of 7.15, an induction time of about 1 h was observed, as the barium concentration remained constant at its initial value of 400 μg/L, dropping thereafter. Fig. 3-b, which displays the $BaSO_4$ supersaturation ratio versus time, shows that even after 45 h the reaction was not complete, since the supersaturation ratio S was much above the equilibrium value of 1. For an initial concentration of 9716 SO_4 mg/L, corresponding to an S value of 8.68, the barium concentration dropped within two minutes or less from 300 μg/L (initial nominal values of concentration and supersaturation are not shown on the graph) to a steady low value of about 30 μg/L, which corresponds to a supersaturation ratio S of 3. It is possible that such residual supersaturation was due to the formation of small crystals of high solubility according to the Gibbs-Thomson effect. Wong et al. [21] have found that smaller barium sulfate crystals are obtained at larger sulfate-to-barium ratios. They have found particle sizes of 20 μm and 3–5 μm when the sulfate-to-barium molar ratio was stoichiometric and 15:1, respectively. In our experiments, this ratio was in excess of 3826:1, so even smaller crystals were likely. Unfortunately, given the extremely low solids concentrations, it was not possible to measure the crystal size.

In Fig. 3 a vastly difference on induction time was observed for the two runs (one with sulfate ion of 1070 and S of 7.15, the other with 9716 mg/L and S of 8.68). The nucleation mechanism might be different in the two supersaturation ratios, but a single mechanism (homogeneous or heterogeneous) might also explain the results, given the exponential dependence of primary nucleation rate with S. Whatever the primary nucleation mechanism, the induction time decreases with the supersaturation. In order to distinguish homogeneous from heterogeneous nucleation, measurements at several supersaturation values would be needed. For $BaSO_4$, homogeneous primary nucleation has been observed only at much larger S values ($S > 23.6$) [34], so it may be assumed that here the mechanism was heterogeneous nucleation.

5.2. Seeding with $BaSO_4$

Seeded $BaSO_4$ precipitation with varying seeds concentration was studied considering a small sulfate reactant addition (initial concentration of 110 mg/L, which is representative of values commonly found in industrial effluents, see experiments A, B and C in Table 2). As seeds were allowed to equilibrate with the solution for 20 min, partial dissolution of the seeds resulted in barium and sulfate initial nominal concentrations of respectively 2073 μg/L and 111 mg/L in solution after the SO_4 reactant addition (see Table 3). The NaCl nominal

Table 3
Initial nominal conditions. Solution concentrations after seeds dissolution, after reactant addition and before precipitation.

Code	SO_4 (mg/L)	Ba (μg/L)	Ca (mg/L)	$BaSO_4$ seed (g/L)	$CaCO_3$ seed (g/L)	$CaSO_4$ seed (g/L)	I (M/M)	$S_{initial}$	SO_4^{2-}/Ba^{2+} (M/M)	Ca^{2+}/Ba^{2+} (M/M)
A, B	111	2073	0	1	0	0	0.013	7.67	77	0
C	111	2073	0	10	0	0	0.013	7.67	77	0
D	111	1386	0	1	0	0	0.003	7.78	114	0
F	1072	2073	0	1	0	0	0.042	16.03	739	0
I	9718	2073	0	1	0	0	0.266	22.83	6703	0
K	1071	330	6.5	0	0.3125	0	0.042	6.37	4638	52
L	2352	362	533.5	0	0	2.5810	0.073	7.32	9288	5060
M	9716	300	0	0	0	0	0.266	8.68	46300	0
N	9716	300	0	0	0	0	0.266	8.68	46300	0
O	1071	400	0	0	0	0	0.042	7.15	3826	0
P	1072	2166	70	1	0	0	0.042	16.09	707	65
Q	1072	2311	215	1	0	0	0.042	16.03	663	2456
R	2374	2277	70	1	0	0	0.081	19.12	1491	800
S	9718	2624	215	1	0	0	0.271	25.41	5295	2456

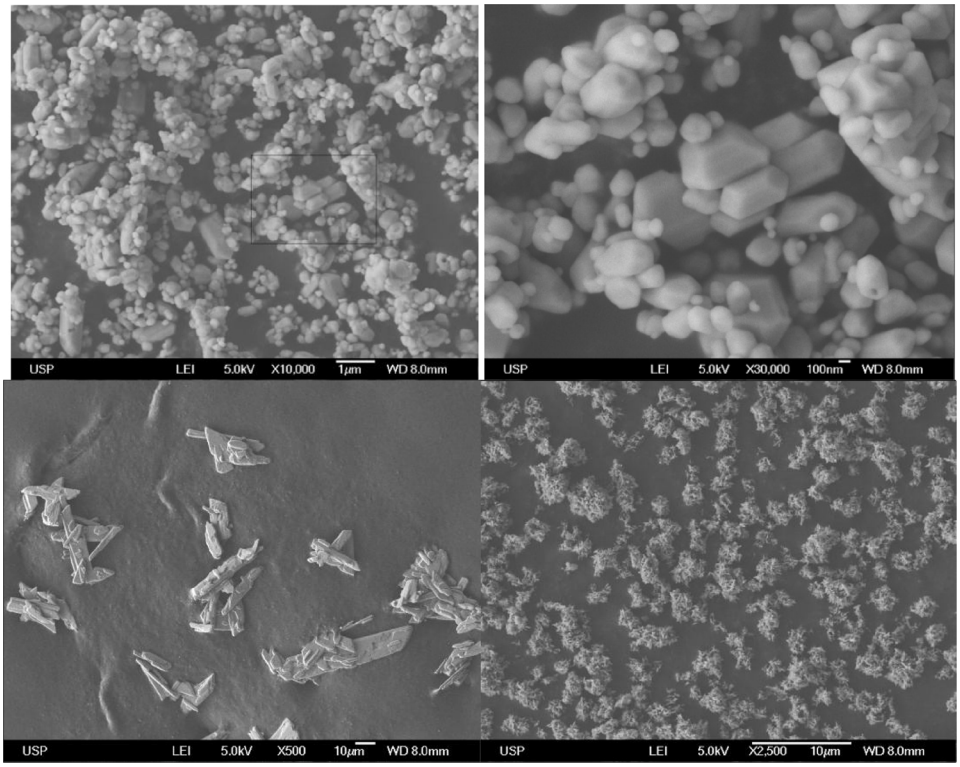

Fig. 2. Scanning Electron Microscopy of seed crystals: $BaSO_4$ (upper left, 10 000 ×); $BaSO_4$ (upper right, 30 000 ×); $CaSO_4$ (lower left, 500 ×) and $CaCO_3$ (lower right, 2500 ×).

concentration was 584 mg/L. Fig. 4a shows that, for 1 g/L seeds, the barium concentration dropped steeply in the first 10 min of reaction and decreased slowly thereafter. The initial nominal value of 2073 μg/L is not given in the figure, only the concentrations after 2.5 min of reaction. Equilibrium was not reached even after 1000s, when the residual supersaturation ratio S was still 1.1 (Fig. 4b). Bremere et al. [11] have obtained a similar residual supersaturation ratio (S = 1.2) for a $BaSO_4$ desupersaturation system consisting of a fixed bed reactor filled with barite seeds with a residence time of 8 min. Kügler et al. [13] have also found that equilibrium was not approached within a monitored time of about 5 h. However, in our experiments with 10 g/L we observed that the concentration drop was faster and that equilibrium was approached within 2.5 min.

Seeded precipitation with various amounts of added SO_4 ions are considered next. The SO_4 initial nominal concentration was in the range of 111–9718 mg/L and the reaction occurred in the presence of 1 g/L of $BaSO_4$ seeds. As before, the NaCl concentration was 584 mg/L and barium initial nominal concentration was 2073 μg/L due to partial seeds dissolution. With the increase on sulfate concentration, the initial drop in soluble barium concentration was faster, as shown in Fig. 5a. A larger excess sulfate also yielded a lower final barium concentration, as expected from the common ion effect. As the sulfate concentration increased, the supersaturation ratio S dropped faster, reaching 1.1 after only 2 min of reaction for the highest sulfate addition (Fig. 5b). In all sulfate additions, the residual supersaturation ratio S of 1.1 was reached after 1000 min. It is possible that the final S was even lower than 1.1, since for concentration values lower than 5 μg/L the ICP analytical quantitative determination becomes less accurate.

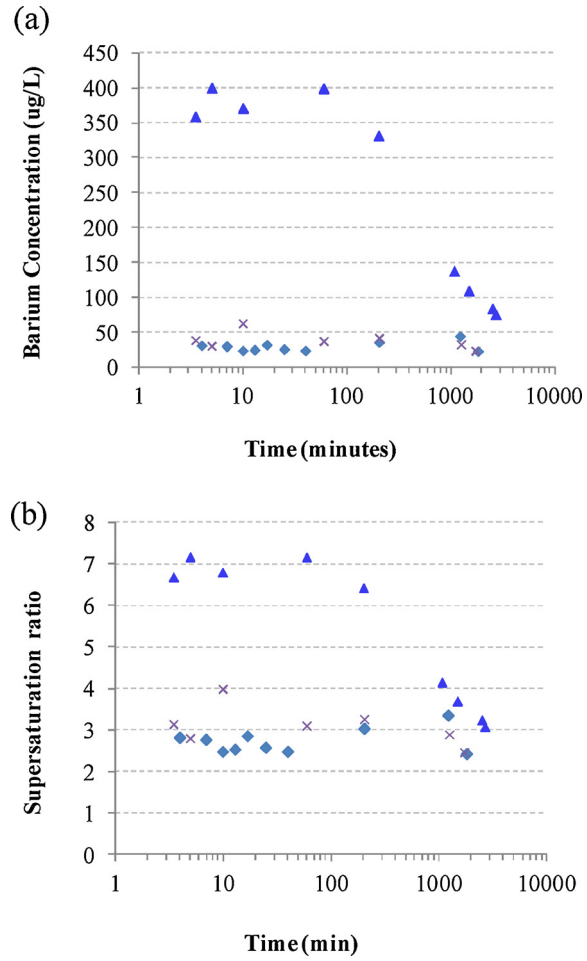

Fig. 3. Barium ion concentration (a) and supersaturation ratio (b) for excess sulfate ion of 1070 (▲) and 9716 (♦, x) mg/L. Unseeded precipitation. Experiments O (▲), N (♦) and M (x).

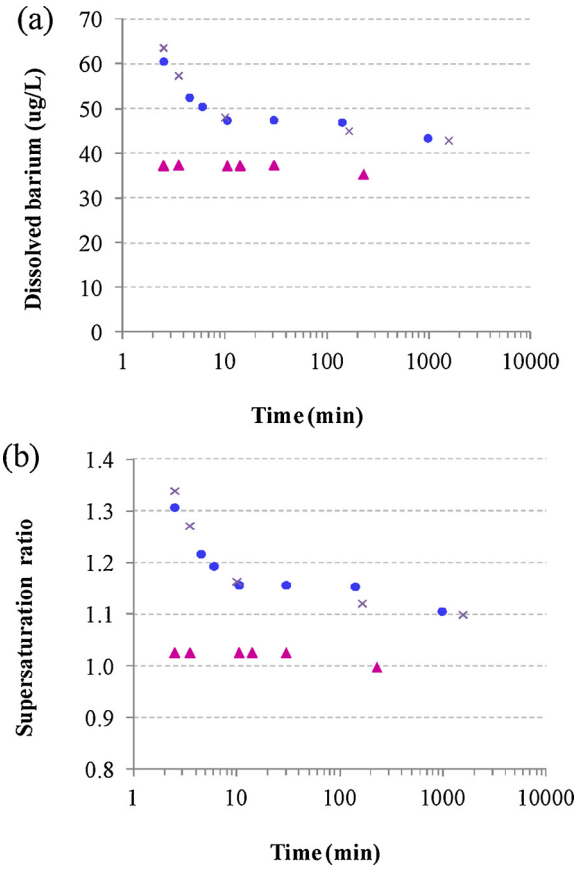

Fig. 4. Barium ion concentration (a) and supersaturation ratio (b) for $BaSO_4$ seeds of 1 g/L (●, x) and 10 g/L (▲). Experiments A (●), B (x) and C (▲).

Comparison between seeded and unseeded precipitation reveals a striking difference. In seeded precipitation an SO_4 initial nominal concentration of only 111 mg/L was sufficient to bring the system close to equilibrium within 2.5 min, whereas in unseeded precipitation more than 1072 mg/L of SO_4 was needed to reach a similar desupersaturation rate.

5.3. Ionic strength

$BaSO_4$ precipitation with varying ionic strength (584 and 0 NaCl mg/L, experiments A, B and D in Tables 2 and 3) is shown in Fig. 6a and b. The reaction occurred in the presence of 1 g/L of $BaSO_4$ seeds. The Ba initial nominal concentrations were respectively 2073 and 1386 μg/L in the presence and absence of NaCl electrolyte. The SO_4 initial nominal concentration was 111 mg/L. The initial supersaturation for the high ionic strength case was slightly lower than for low ionic strength (7.67 and 7.78, respectively).

NaCl electrolyte was found to cause an increase in the soluble barium concentration after precipitation (Fig. 6a). Besides, the solution approached equilibrium at a lower rate (Fig. 6b). Therefore, a high ionic strength resulted in a high $BaSO_4$ solubility and possibly a slower kinetics. The good reproducibility for the high ionic strength conditions (experiments A and B, respectively) suggests that these effects are not due to methodological error. A slower crystal growth at high ionic strength was confirmed by modeling (see Section 6).

5.4. Ca^{2+} ions

$BaSO_4$ precipitation in the presence of varying amounts of Ca^{2+} and SO_4^{2-} ions is shown in Fig. 7 and Tables 2 and 3 (experiments F, P and Q). Thermodynamic modeling showed that gypsum is not formed. In these 1 g/L $BaSO_4$ seeded experiments, the initial nominal sulfate concentration was 1072 mg/L and the NaCl added was adjusted in order to fix the ionic strength with varying $CaCl_2$ addition. Calcium ions were found to inhibit $BaSO_4$ precipitation. For experiments with 70 and 215 mg/L calcium the initial barium concentration dropped from their initial nominal value (of 2073 μg/L) to the approximate value of 200 μg/L within 60 min, whereas in the absence of Ca ions the Ba nominal concentration dropped to 18 μg/L within 2 min (experiment F). Fig. 7b shows the supersaturation ratio S versus time of reaction. Irrespective of the calcium concentration, in the beginning of the reaction the supersaturation dropped rapidly from the starting nominal value S of 16 (not shown in the Figure). It is concluded that calcium ions retard the crystal growth rate for $S > 5$ and virtually block the rate as S approaches a value of 5.

As the sulfate initial nominal concentration increased from 1072 to 2374 (experiments P and R, respectively, in Tables 2 and 3), the soluble barium concentration decreased at the same rate in the first few minutes, as shown in Fig. 8a. This is an unexpected result, given the initial supersaturation also increases with the sulfate concentration (S = 16.1 to 19.1). It appears that calcium more strongly hinders precipitation in larger excess sulfate, possibly because of the lower barium concentration at chemical equilibrium (by the common ion effect), which increases the Ca^{2+}:Ba^{2+} molar ratio. After the first few minutes, the Ba nominal concentration dropped further until, after 180 min of reaction, a steady value of 100 μg/L was reached. This value was lower than the

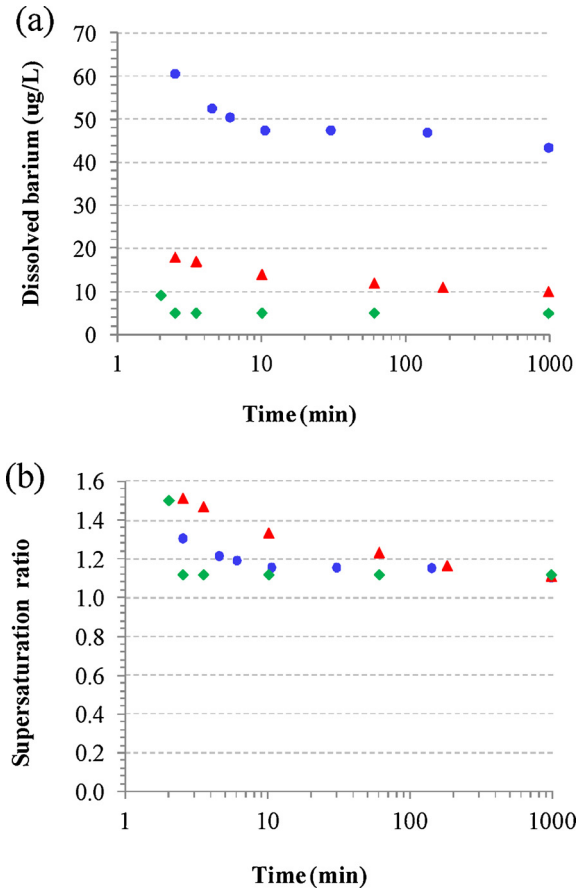

Fig. 5. Barium ion concentration (a) and supersaturation ratio (b) for varying initial nominal sulfate ion concentrations of 111 (●), 1072 (▲) and 9718 (♦) mg/L in the presence of 1 g/L $BaSO_4$ seeds and 584 mg/L added NaCl. Experiments A (●), F (▲) and I (♦).

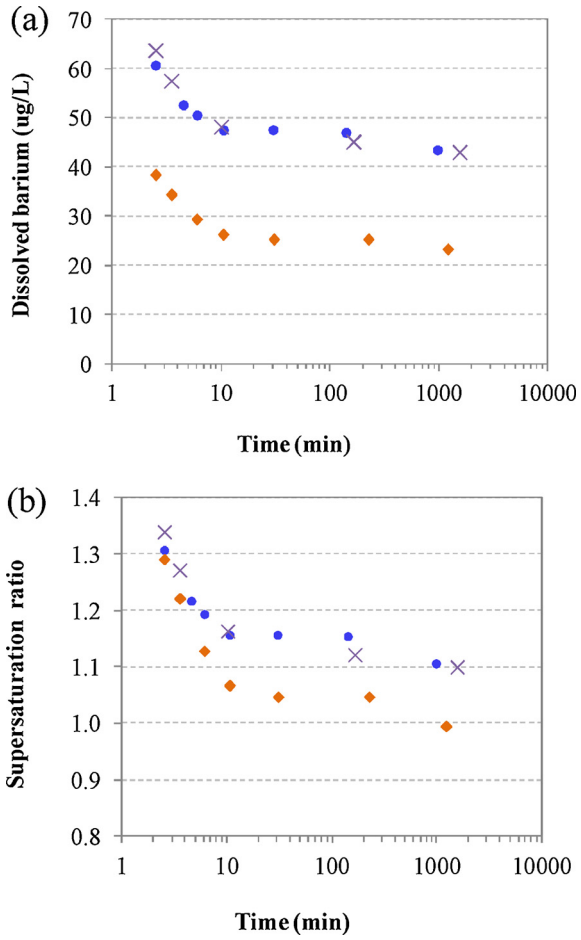

Fig. 6. Barium ion concentration (a) and supersaturation ratio (b) for 584 (●, x) and 0 (♦) mg/L NaCl background electrolyte. $BaSO_4$ seeded experiments with 1 g/L. Experiments A (●), B (x) and D (♦).

one attained from a lower SO_4 addition (final Ba 200 µg/L), as expected from the common ion effect. Fig. 8b shows that the final condition corresponded to a lower residual supersaturation ratio S of 4 (compared to S = 5 for lower sulfate addition).

As the sulfate concentration was further increased from 1072 to 9718 mg/L (experiments Q and S in Tables 2 and 3), just as before, the soluble barium concentration decreased at a lower pace in the first two minutes and continued to drop to a lower value (Fig. 9a). In this case, however, the system approached equilibrium (S = 1) after a few hours (Fig. 9b).

By considering the various calcium and sulfate concentrations described (Figs. 7–9), calcium ions addition resulted in a slower removal of barium ion from solution followed by barium concentration stabilization at a residual supersaturation with respect to barium sulfate. As the initial supersaturation ratio increased (by increasing the sulfate concentration), the residual supersaturation ratio decreased. This behavior may be consequence of primary nucleation at higher supersaturation, which originates an additional crystal surface area of variable surface structure, providing more growth sites and reducing the impact of seed poisoning. For a sufficiently large initial supersaturation, the solution approached equilibrium after 180 min.

We hypothesize that calcium ions reduce the precipitation rate due to calcium adsorption upon barium sulfate surfaces and/or incorporation into the crystal structure, whereas its effects on solubility (by ionic strength increase with $CaCl_2$ addition) are less important. Jones et al. [17] observed the same behavior during $BaSO_4$ precipitation from stoichiometric solutions for calcium concentrations above 50 mg/L.

5.5. Seeding with $CaSO_4{\cdot}2H_2O$ and $CaCO_3$

In an attempt to reduce the cost and the environmental impact of seeding with $BaSO_4$, semi-continuous experiments with heterogeneous seeding were conducted (Tables 2 and 3, experiments K, L and O). Gypsum ($CaSO_4{\cdot}2H_2O$) was chosen because it is abundantly found as industrial construction waste and because it provides free SO_4^{2-} ions upon partial dissolution. The initial concentrations were 362 µg/L of barium and 584 mg/L of NaCl. Calcium and sulfate ion concentrations in solution prior to sulfate addition corresponded to the solubility of gypsum. Speciation modeling yielded a $CaSO_4{\cdot}2H_2O$ solubility of 1.334×10^{-2} M that corresponded to 533 mg/L Ca and 1281 mg/L SO_4. Consequently, after sulfate addition of 1070 mg/L the sulfate initial nominal concentration raised to 2352 mg/L SO_4, leading to an initial nominal supersaturation ratio S of 7.32, which was somewhat higher than in the absence of gypsum seeds (S = 6.70). The time evolution of barium ion concentration and of $BaSO_4$ supersaturation are shown respectively in Fig. 10a and b for both the seeded and unseeded experiments. It reveals that $CaSO_4{\cdot}2H_2O$ heterogeneous seeding did not

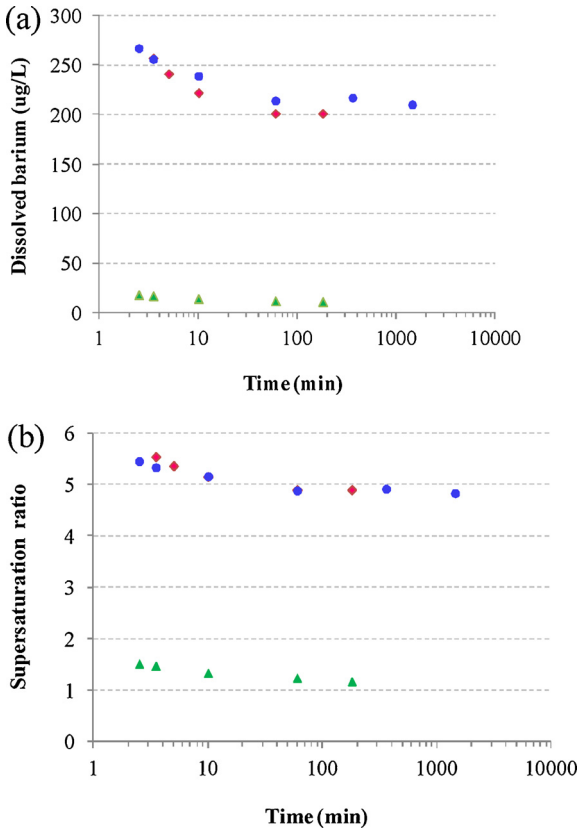

Fig. 7. Barium ion concentration (a) and supersaturation (b) for 70 (♦) and 215 (●) mg/L Ca^{2+} and for no calcium addition (▲). The initial nominal sulfate concentration was 1072, $BaSO_4$ seeded experiments (1 g/L) and fixed ionic strength of I = 0,0416 by varying NaCl addition. Experiments P (♦), Q (●) and F (▲).

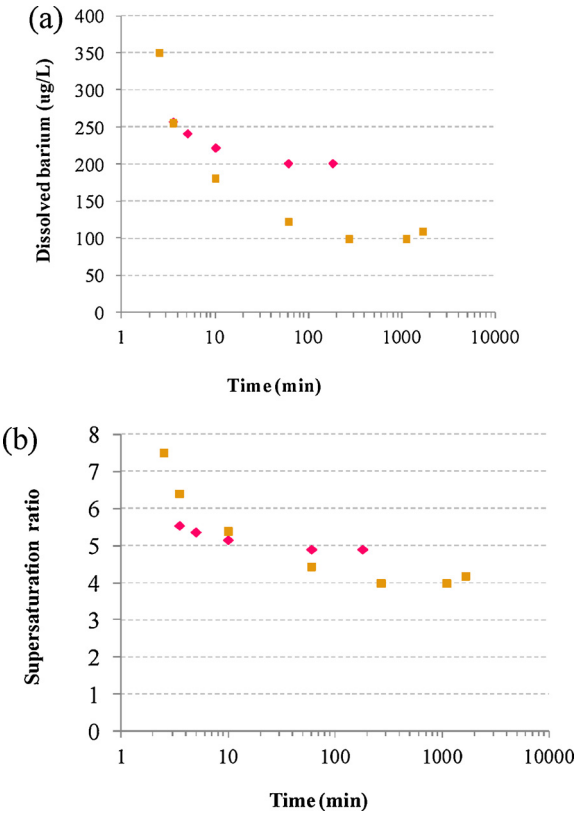

Fig. 8. Barium ion concentration (a) and supersaturation (b) for 70 mg/L Ca^{2+}. The initial nominal sulfate concentration was 1072 (♦) and 2374 mg/L (■), $BaSO_4$ seeded experiments (1 g/L) and NaCl addition of 409 (♦) and 584 (■). Experiments P (♦) and R (■).

substantially increase the rate of $BaSO_4$ precipitation. This result may be explained by recognizing that gypsum is not an effective surface for heterogeneous primary nucleation of $BaSO_4$. A similar behavior has been found by Kügler et al. [13] for silica particles, which were also ineffective heterogeneous seeds for barium sulfate precipitation for supersaturation values up to S of 24.5. It is also possible that the low crystal growth rate associated with calcium ions in solution may have contributed to the ineffectiveness of the gypsum seeds. Finally, one concludes that barium ions adsorption upon gypsum surfaces, which might favor barium removal, is negligible. Isomorphic substitution of barium ions into gypsum lattice, which might also favor barium removal, is unlikely as the solution is only saturated with respect to gypsum.

$CaCO_3$ particles with a calcite structure were also considered as heterogeneous seeds for $BaSO_4$ precipitation, since this material is readily available at low cost and has a large specific surface area (due to a small particle size). For these experiments, the initial concentration was 330 µg/L for barium, 584 mg/L for NaCl and 1070 mg/L for sulfate. Seeds partial dissolution took place prior to sulfate addition. At equilibrium, speciation modeling yielded a pH of 9.89 and 6.5 mg/L Ca. Carbonate and pH measurements in separate experiments with the same reactor (not shown) revealed that the modeling represents well the physics of the systems. Besides, such experiments show that the pH and carbonate concentrations do not change throughout barium sulfate precipitation (because CO_2 absorbed from the air in the reactor headspace is negligible). Fig. 10 shows that, upon the addition of sulfate, an induction period was observed, showing that calcite, just like gypsum, was not an effective surface for heterogeneous primary nucleation of $BaSO_4$. Besides, soluble barium concentration decreases more slowly with time than in the absence of $CaCO_3$ seeds. This may be attributed either to the higher pH of 9.89 (against a pH of 7 in other experiments) or to the presence of 6.5 mg/L Ca^{2+} hampering barium sulfate crystal growth. Finally, one concludes that barium ions adsorption upon calcite surfaces, which might favor barium removal, is negligible. Isomorphic substitution of barium ions into calcite lattice, which might also favor barium removal, is unlikely as the solution is only saturated with respect to calcite.

6. Precipitation simulations

$BaSO_4$ semi-continuous precipitation was simulated for various sulfate-to-barium ratios, seed loads and ion strength values using the same conditions of the experiments A, C, D, F and I given in Table 2. Only seeded experiments were considered to comply with the hypothesis of negligible primary nucleation. In summary, the initial volume of solution inside the reactor V_{sol} was 400 mL, the $BaCl_2$ concentration was 2.73×10^{-6} M. In some experiments 1.25×10^{-2} M NaCl was added. Additionally, 0.5 or 5 g of $BaSO_4$ seeds were added and allowed to partially dissolve until equilibrium, which corresponded to 2073 µg/L dissolved barium. Thereafter the total volume of suspension was gradually increased with the addition of 0.83 mL/s Na_2SO_4 reactant until a final volume of 100 mL. The Na_2SO_4 concentration was adjusted

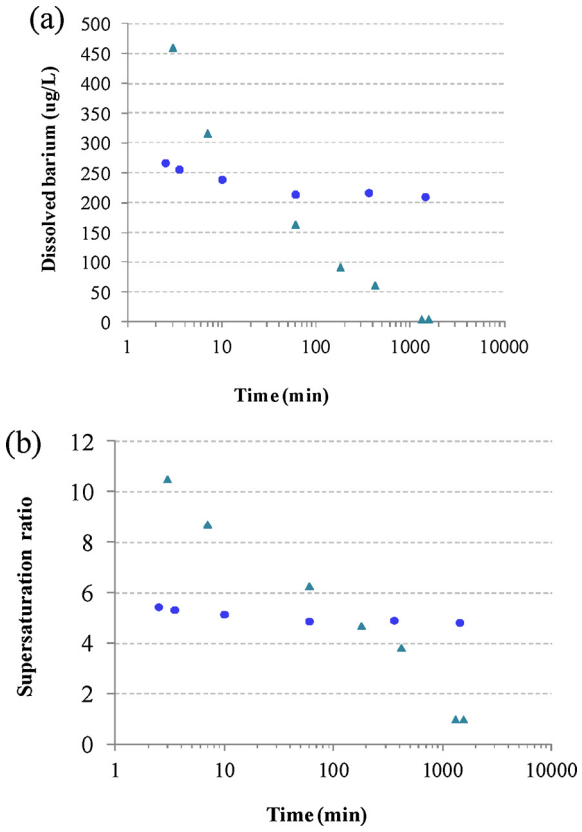

Fig. 9. Barium ion concentration (a) and supersaturation ratio (b) for 215 mg/L Ca^{2+}. $BaSO_4$ seeded experiments (1 g/L). Sulfate concentration was 1072 (●) and 9718 (▲). Experiments Q (●) and S (▲).

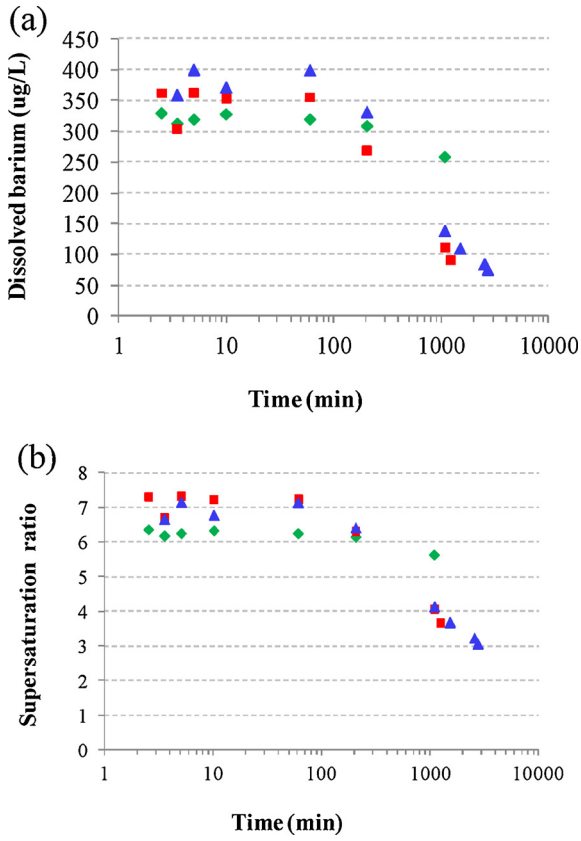

Fig. 10. Barium ion concentration (a) and supersaturation ratio (b) for $CaSO_4.2H_2O$ seeds (■), $CaCO_3$ seeds (♦), and seed absence (▲). Initial sulfate concentration 1070 mg/L. Experiments L (■), K (♦) and O (▲).

to yield initial nominal concentrations of 111, 1072 or 9718 mg/L SO_4.

In each time interval Δt of 0.6s, the moments of the particle size distribution ($m_0(t)$, $m_1(t)$, $m_2(t)$ and $m_3(t)$) and the components concentrations in solution (C_{Ba}, C_{SO4}, C_{Na} and C_{Cl}) were recalculated, considering the barium sulfate crystal growth rate and the speciation of barium and sulfate ions in solution. For each time interval, the supersaturation ratio S was determined and used to calculate the crystal growth rate.

A fourth order crystal growth rate (g = 4) was the best fit to the experimentally determined barium concentrations. Such a high order might be caused by impurities hampering growth. However, impurities in these experiments are estimated to be in concentrations of a few parts per billion or less, making this hypothesis unlikely. Therefore, one concludes that the high crystal growth order was caused by the growth mechanism of superficial 2-D nucleation, as was observed elsewhere [43,27,39].

The growth rate parameter k_g found for 111, 1072 and 9718 mg/L sulfate were respectively 5×10^{-12}, 4×10^{-13} and 6×10^{-13} m/s. The growth parameters thus decreased one order of magnitude and then stabilized as the excess sulfate increased. Such decreasing value of k_g with an increasing SO_4/Ba molar ratio was first reported by Boerlage et al. [15]. The model simulations and the experimental results are compared in Fig. 11. Fig. 11a shows the dissolved barium and Fig. 11b, the $BaSO_4$ supersaturation ratio over the reaction time. The high order g = 4 explains why the barium removal did not progress until chemical equilibrium for seeds concentration of 1 g/L, giving rise to a residual supersaturation higher than 1.1 (Fig. 11b) for all of the initial nominal sulfate concentrations.

The model did not fit the data appropriately for the highest sulfate addition. It is hypothesized that this difference was caused by primary nucleation, which was not taken into account in the model. In this simulation, the supersaturation ratio reached a value of 7.3 (Fig. 11b), which was the highest among all conditions investigated. Besides, this supersaturation value might be sufficient to trigger primary nucleation, as our unseeded experiments suggest. In these experiments (Fig. 3), a supersaturation ratio of 7.15 yielded a long induction time, whereas an S value of 8.68 resulted in instantaneous nucleation.

The model simulations and the experimental results for two ionic strengths are shown in Fig. 12. For the higher ionic strength the concentration after 100 min precipitation time was higher, which may be explained by the correspondingly higher solubility (not shown). A fourth order crystal growth rate was found with k_g of 5×10^{-12} and 1×10^{-11} for the higher and the lower ionic strength respectively, suggesting that the ionic strength also reduced the crystal growth rate.

Precipitation kinetics for seeds concentrations of 1 and 10 g/L are also shown in Fig. 12. A reasonable fit was found with the parameters just described. For 10 g/L the simulations showed a small delay when compared to the experimental results but represented well the low supersaturation (S = 1.02) found at later stages. Therefore, both model and experiments showed that increasing the superficial area of the seeds is a suitable tool to rapidly approach saturation.

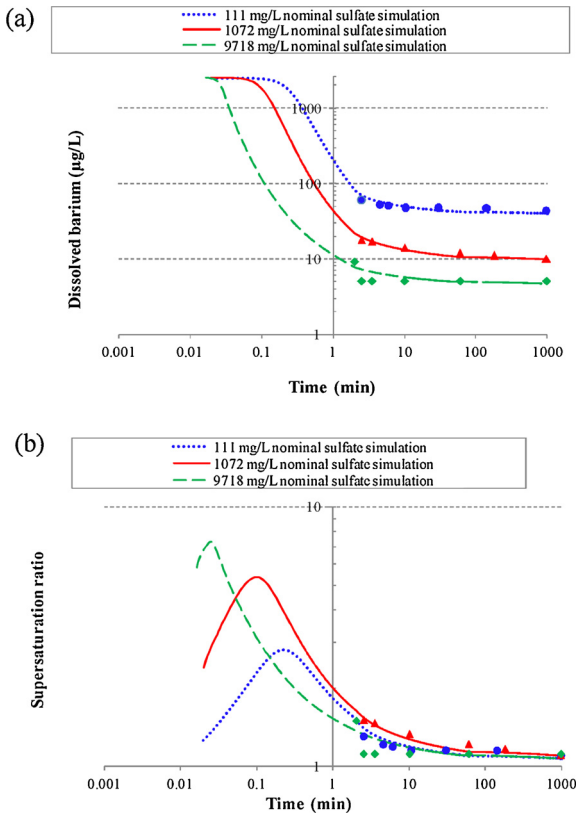

Fig. 11. Simulation of barium precipitation by seeds growth for varying initial nominal sulfate concentrations of 111 (●), 1072 (▲) and 9718 (♦) mg/L. Barium ion concentration (a) and supersaturation ratio (b) in the presence of 1 g/L $BaSO_4$ seeds and 584 mg/L NaCl. Lines are simulation results and data points are from experiments A (●), F (▲) and I (♦).

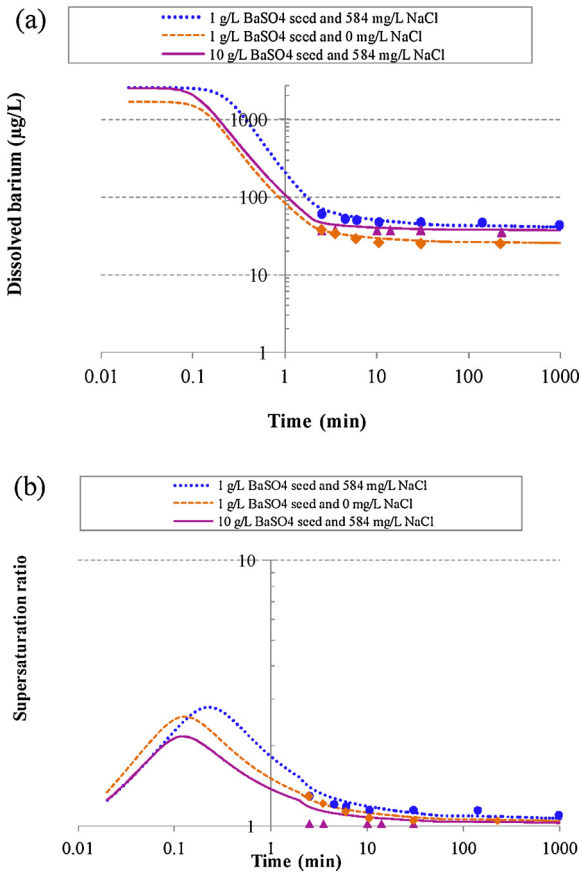

Fig. 12. Simulation of barium precipitation by seeds growth for seeds addition of 1 (●, ♦) and 10 g/L (▲), and with 584 (●, ▲) and 0 (♦) mg/L of NaCl. Barium ion concentration (a) and supersaturation ratio (b). The sulfate nominal concentration was 111 mg/L. Lines are simulations and data points are experimental values from A (●), C (▲) and D (♦).

7. Conclusions

Barium removal from synthetic solutions of a typical industrial wastewater composition was studied by batchwise addition of excess sulfate. An induction time of a few hours is observed for an initial nominal supersaturation ratio S of 7.15 or lower (excess sulfate of 1072 mg/L SO_4 or lower). By increasing S to 8.7 (9716 mg/L SO_4), primary nucleation and crystal growth proceeds within a few minutes, but a residual S of about 3 remains for a few hours. Seeding with $CaCO_3$ or $CaSO_4{\cdot}2H_2O$ does not accelerate precipitation, showing that these compounds do not act as heterogenous seeds for $BaSO_4$ precipitation. By seeding with $BaSO_4$, on the contrary, barium residual supersaturation is greatly reduced in a few minutes of reaction. For a low seeds concentration of 1 g/L, a residual S of 1.1 remains for a few hours, whereas for 10 g/L seeds equilibrium is approached within a few minutes. In seeded precipitation an SO_4 initial nominal concentration of only 111 mg/L (S of 7.7) is sufficient to bring the system close to equilibrium within 2.5 min, whereas in unseeded precipitation more than 1072 mg/L of SO_4 (S of 8.7) is needed to reach a similar desupersaturation rate.

Calcium ions retard the removal of barium ions from solution and blocks the process at a high residual S with respect to barium sulfate ($4 < S < 5$). As the initial S increases, the residual S decreases. For a sufficiently large initial S (of 25.4), the solution approaches equilibrium after 180 min. We have also found that calcium more strongly hinders the precipitation process as the excess sulfate increases in the range of 111–9718 mg/L SO_4^{2-}. We hypothesize that calcium ions reduce the precipitation rate due to calcium adsorption upon barium sulfate surfaces and/or incorporation into the crystal structure, whereas their effects on solubility are less important.

Kinetic modeling of batchwise seeded precipitation of barium sulfate has shown that barium sulfate crystal growth is 4th order with respect to the supersaturation ratio S, consistent with a 2D nucleation growth mechanism. Such high order explains the observed residual supersaturation ratio values higher than 1.1. The growth rate decreases with an increasing SO_4/Ba molar ratio. The ionic strength slows down the crystal growth rate and enhances the solubility of barium sulfate.

Acknowledgements

The authors gratefully acknowledge Petrobras for the financial support [FUSP, 2913] and the National Council for Scientific and Technological Development for the scholarships.

References

[1] Dow Chemical Company, Technical Manual FILMTEC™ Reverse Osmosis Membranes, (2011) pp 181 http://msdssearch.dow.com/PublishedLiteratureDOWCOM/dh_095b/0901b8038095b91d.pdf?filepath=liquidseps/pdfs/noreg/609-00071.pdf.

[2] A. Rahardianto, J.B. Gao, C.J. Gabelich, M.D. Williams, Y. Cohen, High recovery membrane desalting of low-salinity brackish water: integration of accelerated precipitation softening with membrane RO, J. Membr. Sci. 289 (1-2) (2007) 123–137.

[3] R.Y. Ning, A. Tarquin, M.C. Trzcinski, G. Patwardhan, Recovery optimization of RO concentrate from desert wells, Desalination 201 (1–3) (2006) 315–322.

[4] S.E.H. Comstock, T.H. Boyer, K.C. Graf, Treatment of nanofiltration and reverse osmosis concentrates: comparison of precipitative softening, coagulation, and anion exchange, Water Res. 45 (16) (2011) 4855–4865.
[5] C.J. Gabelich, M.D. Williams, A. Rahardianto, J.C. Franklin, Y. Cohen, High-recovery reverse osmosis desalination using intermediate chemical demineralization, J. Membr. Sci. 301 (1–2) (2007) 131–141.
[6] C. Gabelich, A. Rahardianto, C. Northrup, T. Yun, Y. Cohen, Process evaluation of intermediate chemical demineralization for water recovery enhancement in production-scale brackish water desalting, Desalination 272 (1–3) (2011) 36–45.
[7] R. Bond, S. Veerapaneni, Zeroing in on ZLD technologies for inland desalination, J. Am. Water Works Assn. 100 (9) (2008) 76–89.
[8] A. Tesoriero, J. Pankow, Solid solution partitioning of Sr^{2+}, Ba^{2+}, and Cd^{2+} to calcite, Geochim. Cosmochim. Acta 60 (6) (1996) 1053–1063.
[9] R. Reeder, Interaction of divalent cobalt, zinc, cadmium, and barium with the calcite surface during layer growth, Geochim. Cosmochim. Acta 60 (9) (1996) 1543–1552.
[10] J. Astilleros, C. Pina, L. Fernandez-Diaz, M. Prieto, A. Putnis, Nanoscale phenomena during the growth of solid solutions on calcite {1014} surfaces, Chem. Geol. 225 (2006) 322–335.
[11] I. Bremere, M.D. Kennedy, A. Johnson, R. van Emmerik, G.J. Witkamp, J.C. Schippers, Increasing conversion in membrane filtration systems using a de-supersaturation unit to prevent scaling, Desalination 119 (1–3) (1998) 199–204.
[12] I. Bremere, M. Kennedy, P. Michel, R. van Emmerik, G.J. Witkamp, J. Schippers, Controlling scaling in membrane filtration systems using a desupersaturation unit, Desalination 124 (1–3) (1999) 51–62.
[13] R.T. Kügler, K. Beißert, M. Kind, On heterogeneous nucleation during the precipitation of barium sulfate, Chem. Eng. Res. Des. 114 (2016) 30–38.
[14] S.F.E. Boerlage, M.D. Kennedy, G.J. Witkamp, J.P. van der Hoek, J.C. Schippers, $BaSO_4$ solubility prediction in reverse osmosis membrane systemsBaSO4 solubility prediction in reverse osmosis membrane systems, J. Membr. Sci. 159 (1–2) (1999) 47–59.
[15] S.F.E. Boerlage, M.D. Kennedy, I. Bremere, G.J. Witkamp, J.P. van der Hoek, J.C. Schippers, Stable barium sulphate supersaturation in reverse osmosis, J. Membr. Sci. 179 (1–2) (2000) 53–68.
[16] F. Jones, A. Oliviera, G. Parkinson, A. Rohl, A. Stanley, T. Upson, The effect of calcium cations on the precipitation of barium sulfate 2: calcium ions in the presence of organic additives, J. Cryst. Growth 270 (3–4) (2004) 593–603.
[17] F. Jones, A. Oliviera, G. Parkinson, A. Rohl, A. Stanley, T. Upson, The effect of calcium ions on the precipitation of barium sulphate 1: calcium ions in the absence of organic additives, J. Cryst. Growth 262 (1–4) (2004) 572–580.
[18] A. Hennessy, G. Graham, The effect of additives on the co-crystallisation of calcium with barium sulphate, J. Cryst. Growth 237 (2002) 2153–2159.
[19] M. Kelland, Effect of various cations on the formation of calcium carbonate and barium sulfate scale with and without scale inhibitors, Ind. Eng. Chem. Res. 50 (9) (2011) 5852–5861.
[20] S. Redfern, S. Parker, Atomistic simulation of the effects of calcium and strontium defects on the surface structure and stability of BaSO4, J. Chem. Soc. Faraday Trans. 94 (14) (1998) 1947–1952.
[21] D. Wong, Z. Jaworski, A. Nienow, Effect of ion excess on particle size and morphology during barium sulphate precipitation: an experimental study, Chem. Eng. Sci. 56 (3) (2001) 727–734.
[22] R.B. Fischer, T.B. Rhinehammer, Rapid precipitation of barium sulfate, Anal. Chem. 25 (10) (1953) 1544–1548.
[23] M. Kucher, D. Babic, M. Kind, Precipitation of barium sulfate: experimental investigation about the influence of supersaturation and free lattice ion ratio on particle formation, Chem. Eng. Process. 45 (10) (2006) 900–907.
[24] M. Kucher, T. Beierlein, M. Kind, In situ WAXS synchrotron radiation study on particle formation of precipitated barium sulfate, AIChE J. 54 (5) (2008) 1178–1188.
[25] C. Steyer, K. Sundmacher, Impact of feeding policy and ion excess on particle shape in semi-batch precipitation of barium sulfate, J. Cryst. Growth 311 (2009) 2702–2708.
[26] M. Aoun, E. Plasari, R. David, J. Villermaux, Are barium sulphate kinetics sufficiently known for testing precipitation reactor models? Chem. Eng. Sci. 51 (10) (1996) 2449–2458.
[27] G.H. Nancollas, N. Purdie, Crystallization of barium sulphate in aqueous solution, Trans. Faraday Soc. 59 (483) (1963) 735.
[28] C. Steyer, M. Mangold, K. Sundmacher, Modeling of particle size distribution for semibatch precipitation of barium sulfate using different activity coefficient models, Ind. Eng. Chem. Res. 49 (2010) 2456–2468.
[29] R.T. Kügler, S. Doyle, M. Kind, Fundamental insights into barium sulfate precipitation by time-resolved in situ synchrotron radiation wide-angle X-ray scattering (WAXS), Chem. Eng. Sci. 133 (2015) 140–147.
[30] J.N. Bracco, Y. Gooijer, S.R. Higgins, Hydrothermal atomic force microscopy observations of barite step growth rates as a function of the aqueous barium-to-sulfate ratio, Geochim. Cosmochim. Acta 183 (2016) 1–13.
[31] L. Metzger, M. Kind, The influence of mixing on fast precipitation processes − A coupled 3D CFD-PBE approach using the direct quadrature method of moments (DQMOM), Chem. Eng. Sci. 169 (2017) 284–298.
[32] NIST 46.7, National Institute of Standards and Technology Reference Databases, (2014).
[33] A.A. Oncul, K. Sundmacher, D. Thevenin, Numerical investigation of the influence of the activity coefficient on barium sulphate crystallization, Chem. Eng. Sci. 60 (19) (2005) 5395–5405.
[34] L. Vicum, M. Mazzotti, J. Baldyga, Applying a thermodynamic model to the non-stoichiometric precipitation of barium sulfate, Chem. Eng. Technol. 26 (3) (2003) 325–333.
[35] A.E. Lewis, M.M. Seckler, H. Kramer, G.M. van Rosmalen, Industrial Crystallization: Fundamentals and Applications, Cambridge University Press, Cambridge, UK, 2015, p. 346.
[36] W.G. Cobbett, C.M. French, The precipitation of barium sulphate from aqueous solutions, Discuss. Faraday Soc. 18 (1954) 113–119.
[37] A.E. Nielsen, Electrolyte crystal-growth mechanisms, J. Cryst. Growth 67 (2) (1984) 289–310.
[38] M. van Leeuwen, Precipitation and Mixing, Delft University of Technology, Mekelweg 4, 2628 CA Delft, The Netherlands, 1998.
[39] S.T. Liu, G.H. Nancollas, E.A. Gasiecki, Kinetic studies scanning electron-microscopic and of crystallization and dissolution of barium sulfate crystals, J. Cryst. Growth 33 (1) (1976) 11–20.
[40] R.H. Doremus, Crystallization of slightly soluble salts from solution, J. Phys. Chem. 74 (7) (1970) 1405–1408.
[41] M.C. van der Leeden, D. Kashchiev, G.M. van Rosmalen, Precipitation of barium sulfate: induction time and the effect of an additive on nucleation and growth, J. Colloid Interface Sci. 152 (2) (1992) 338–350.
[42] D. Gunn, M. Murthy, Kinetics and mechanisms of precipitations, Chem. Eng. Sci. 27 (6) (1972) 1293–1313.
[43] A.E. Nielsen, The kinetics of crystal growth in barium sulfate precipitation. 2. Temperature dependence and mechanism, Acta Chem. Scand. 13 (4) (1959) 784–802.
[44] K. Taguchi, J. Garside, N.S. Tavare, Nucleation and growth kinetics of barium sulphate in batch precipitation, J. Cryst. Growth 163 (3) (1996) 318–328.